Nucleic Acids Research, 1998, Vol. 26, No. 16 **3837–3844**

2-Aminopurine fluorescence studies of base stacking interactions at abasic sites in DNA: metal-ion and base sequence effects

James T. Stivers*

Center for Advanced Research in Biotechnology, University of Maryland, Biotechnology Institute and the National Institute for Standards and Technology, 9600 Gudelsky Drive, Rockville, MD 20850, USA

Received March 12, 1998; Revised and Accepted June 30, 1998

ABSTRACT

Metal-ion and sequence dependent changes in the stacking interactions of bases surrounding abasic (AB) sites in 10 different DNA duplexes were examined by incorporating the fluorescent nucleotide probe 2-aminopurine (2-AP), opposite to the site (AB-AP^{opp}) or adjacent to the site (AB-AP^{adj}) on either strand. A detailed study of the fluorescence emission and excitation spectra of these AB duplexes and their corresponding parent duplexes indicates that AB-AP^{opp} is significantly less stacked than 2-AP in the corresponding normal duplex. In general, AB-AP^{adj} on the AB strand is stacked, but AB-AP^{adj} on the opposite strand shows destabilized stacking interactions. The results also indicate that divalent cation binding to the AB duplexes contributes to destabilizaton of the base stacking interactions of AB-AP^{opp}, but has little or no effect on the stacking interactions of AB-AP^{adj}. Consistent with these results, the fluorescence of AB-AP^{opp} is 18–30-fold more sensitive to an externally added quenching agent than the parent normal duplex. When uracil DNA glycosylase binds to AB-AP^{opp} in the presence of 2.5 mM $MgCl_2$, a 3-fold decrease in fluorescence is observed (K_d = 400 ± 90 nM) indicating that the unstacked 2-AP^{opp} becomes more stacked upon binding. On the basis of these fluorescence studies a model for the local base stacking interactions at these AB sites is proposed.

INTRODUCTION

Abasic sites in DNA (AB-DNA) can arise from the action of DNA repair glycosylases or various chemical processes (1). For instance, the spontaneous hydrolysis of the purine glycosidic bond has been estimated to generate ~10^4 AB sites per cell cycle in humans (2). Thus, AB sites occur frequently in cellular DNA, and structural knowledge of such sites is important for understanding how repair enzymes recognize and repair these lesions (3–6).

Extant structural information on AB sites has largely come from nuclear magnetic resonance studies of apyrimidinic or apurinic sites in small oligonucleotides (7–14). An interesting aspect arising from these studies is whether the base facing the AB site is intrahelical or extrahelical. When adenine faces the AB site, it is found to stack inside the helix regardless of the nature of the residues flanking the AB site (8). When guanine faces the site, it is found in a dynamic equilibrium between an intra- and extrahelical conformation (8). When a pyrimidine faces the AB site, and the site is flanked by purine residues, then the pyrimidine is found in an extrahelical conformation, or a dynamic equilibrium between an intra- and extrahelical conformation (8). Contrastingly, when the AB site is flanked by two pyrimidines, the pyrimidine opposite to the site is found in a stacked conformation (14). Thus, these NMR studies performed in the *absence* of divalent cations suggest a high degree of flexibility at AB sites, and that the conformation of the site is highly dependent on base facing the site and the interaction energies between nucleotides flanking the site.

Although NMR is a high-resolution method for elucidation of stable conformations of oligonucleotides, it is often difficult to detect transient structures using NMR, or conformers that are in dynamic equilibrium. Therefore, other approaches, such as fluorescence spectroscopy, can often provide complementary structural and dynamic information. A useful fluorescent reporter group is 2-aminopurine deoxyribonucleoside (2-AP) which can be incorporated into specific sites in DNA using phosphoramidite solid-phase synthetic methods. The quantum yield of 2-AP is very sensitive to its environment, and exhibits strong quenching when AP is stacked in duplex DNA (15). Thus, 2-AP has been used extensively to study the dynamics and structure of specific sites in DNA and to monitor interactions of enzymes with DNA (16–18). Recently, 2-aminopurine riboside has also been used to study Mg^{2+}-dependent conformational changes in the hammerhead ribozyme (19).

In this study, I report on the effects of metal ions on the base stacking interactions at several AB sites, by monitoring the fluorescence spectra of a 2-AP base located both opposite and adjacent to these sites, and the sensitivity of the fluorescence to external quenching agents. These results indicate that physiological concentrations of divalent cations destabilize the local stacking interactions at these AB sites, with the largest effect seen when the

*Tel: +1 301 738 6264; Fax: +1 301 738 6255; Email: stivers@carb.nist.gov

2-AP base is located *opposite* to the site. This effect was found to be largely independent of the base sequence surrounding the site. When the repair enzyme uracil DNA glycosylase (UDG) binds to the AB DNA, the unstacked 2-AP base re-stacks inside the helix, suggesting that such conformational changes may occur when other DNA repair enzymes bind AB sites. [The term 'unstacked', as used in this paper, refers to all possible conformations of 2-AP^{opp} (2-aminopurine base located opposite to the AB site) that could lead to its altered spectroscopic properties as compared to normal duplex DNA. The spectra indicate that 2-AP^{opp} is in a unique, temperature dependent conformation with increased solvent exposure, increased sensitivity to quenching agents and decreased excitation energy transfer from adjacent bases. These spectral qualities indicate decreased stacking interactions.] This work suggests a model for the relative stacking interactions near AB sites, and provides the foundation for transient fluorescence studies of the dynamics of these AB sites, both free in solution and bound to enzymes.

MATERIALS AND METHODS

Enzymes and reagents

Escherichia coli UDG was over-produced using a T7 polymerase based expression system (Novagen, Inc.) and purified essentially as described (20). [Certain commercial equipment, instruments and materials are identified in this paper in order to specify the experimental procedure. Such identification does not imply recommendation or endorsement by the National Institute of Standards and Technology, nor does it imply that the material or equipment identified is necessarily the best available for the purpose.] All other enzymes and reagents were of the highest quality available from commercial sources.

Oligodeoxynucleotide synthesis

Oligodeoxyribonucleotides were synthesized using an Applied Biosystems 390 synthesizer using standard phosphoramidite chemistry. The nucleoside phosphoramidites were purchased from Applied Biosystems or Glen Research (Sterling, VA). After synthesis, oligonucleotides were purified by either reverse-phase HPLC with the trityl group attached, (PRP-1 column, Hamilton) or anion-exchange HPLC with the trityl group removed, (Zorbax Oligo column, Rockland Technologies, Inc.). The oligonucleotides purified by anion-exchange chromatography were desalted using Sephadex G-25 gel-filtration chromatography using water as the eluent. The size and purity of the DNA was assessed by denaturing polyacrylamide gel electrophoresis with visualization by ^{32}P radiolabeling or ethidium bromide staining. The concentrations were determined by UV absorption measurements at 260 nm, using the pairwise extinction coefficients for the constituent nucleotides (21). The oligonucleotides used in these studies are shown in Table 1.

Hybridization of duplex DNA

Duplex DNA molecules (Table 1) were hybridized from equimolar amounts of the respective single-strand oligonucleotides in TN buffer (20 mM Tris–HCl pH 8.0, 60 mM NaCl and 0.1 mM EDTA). Samples were heated to 70°C followed by slow cooling to room temperature over at least 2 h. To confirm that the DNA was in the duplex form and that the stoichiometry for the strands was 1:1, native polyacrylamide gel electrophoresis was performed followed by staining with ethidium bromide. The melting temperatures for many of these duplexes were measured, and fell in the range 56 ± 1°C for the normal duplexes, and ~ 6°C lower for the AB forms (TMN buffer, $\Delta T/\Delta t = 1$°C/min, [duplex] = 1 μM). Thus, at the temperatures and concentrations used in this work both the normal and AB DNA molecules are in the duplex form. CD spectra were obtained using a JASCO J-720 spectropolarimeter at a duplex concentration of 5 μM in TN buffer containing varying concentrations of $MgCl_2$. A cell with a 1 cm path length was used.

Continuous fluorescence kinetic assay for UDG activity

UDG activity was measured by following the fluorescence increase of a 2-aminopurine base that was incorporated opposite to the excised uracil in the duplex DNA substrate. The initial velocity (in units of M/s) was calculated by measuring the initial linear slope of the fluorescence increase (in units of F/s), and then dividing by the constant $a = \Delta F/[S]_{tot}$, where ΔF is the maximal change in F and S_{tot} is the total substrate concentration used in a given reaction. The rates and kinetic parameters measured using this assay have been shown to be indistinguishable from a radioactivity-based assay (not shown).

Preparation of aldehydic AB DNA

Two types of AB DNA molecules were used in these studies. The first is the synthetic tetrahydrofuran AB site analog that may be incorporated during solid phase oligonucleotide synthesis using phosphoramidite chemistry (Table 1). The second AB site is the naturally occurring aldehydic form, which was prepared by treatment of deoxyuridine-containing duplex oligonucleotides (1 μM) with UDG (0.5–1 nM) in TN buffer at 25°C for at least 1 h. The reaction was determined to be complete by monitoring the fluorescence increase of the 2-AP base accompanying glycosidic bond cleavage (see Results), or by 5′-^{32}P labeling of the uracil strand followed by thermal cleavage of the AB sites and analysis by gel electrophoresis (3). It was not necessary to remove the trace amount of glycosylase or free uracil from the AB DNA product, because the contribution from the enzyme fluorescence is negligible, and identical fluorescence spectra were obtained with HPLC purified aldehydic AB DNA samples, as well the tetrahydrofuran AB site analog (not shown).

Steady-state fluorescence measurements

Steady-state fluorescence emission spectra of the AP-containing oligodeoxynucleotide samples were measured on a SPEX Fluoromax spectrofluorometer using a 3 mm square cuvette. The emission spectra were recorded over the wavelength range 330–450 nm with an excitation wavelength of 310 nm. The spectral bandpass was 4 nm for all emission spectra. The excitation spectra were recorded over the wavelength range 240–330 nm by monitoring the emission 370 nm. No corrections for inner filter effects were necessary because the maximal absorbance at each excitation wavelength was always <0.1.

Binding measurements

The apparent binding constants for divalent cation binding to the AB DNA molecules were determined by monitoring the increase in fluorescence (F) of the AP base using equation **1**, which describes binding to a single class of sites. In this analysis, the

Table 1. Sequences of the single- and double-stranded oligonucleotides used in this study and fluorescence properties

Abbreviation	DNA Sequence	λ^{ex}_{max} (nm)[b]	$\Delta\lambda^{ex}_{max}$ (nm)[c]	F_{AB}/F_{dup}[d]
I. ss**P**[e]	5′GCGCTTTTT**P**TTTGGCCGC3′	308 (308)	-	-
II. **P** opposite to site, AT-rich duplex				
a.) AUA/T**P**T (Y = U[f])	5′GCGGCCAAAYAAAAAGCGC3′ 3′CGCCGGTTT**P**TTTTTCGCG5′	317 (317)	-	-
b.) A*D*A/T**P**T (Y = *D*[g])		311 (309)	-6 (-8)	1.58 (5.88)
c.) ATA/T**P**T (Y = T)		319 (319)	-	-
d.) A*F*A/T**P**T (Y = *F*[h])		314 (311)	-5 (-8)	1.23 (5.86)
III. **P** opposite to site, G or C flanking site				
a.) GUG/C**P**C (Y = U)	5′GCGGCCAAGYGAAAAGCGC3′ 3′CGCCGGTTC**P**CTTTTCGCG5′	309 (309)	-	-
b.) G*D*G/C**P**C (Y = *D*)		308 (308)	-1 (-1)	2.28 (8.03)
c.) CUC/G**P**G (Y = U)	5′GCGGCCAACYCAAAAGCGC3′ 3′CGCCGGTTG**P**GTTTTCGCG5′	309 (309)	-	-
d.) C*D*C/G**P**G (Y = *D*)		309 (308)	0 (-1)	1.62 (5.8)
IV. **P** adjacent to site				
a.) **P**UA/TAT (Y = U)	5′GCGGCCAA**P**YAAAAAGCGC3′ 3′CGCCGGTTTATTTTTCGCG5′	312 (312)	-	-
b.) **P***D*A/TAT (Y = *D*)		315 (315)	3 (3)	2.67 (3.14)
c.) AU**P**/TAT (Y = U)	5′GCGGCCAAAY**P**AAAAGCGC3′ 3′CGCCGGTTTATTTTTCGCG5′	315 (314)	-	-
d.) A*D***P**/TAT (Y = *D*)		314 (315)	-0.5 (0)	1.2 (1.43)
V. **P** adjacent to site on opposite strand				
a.) AUT/**P**AT (Y = U)	5′GCGGCCAAAYTAAAAGCGC3′ 3′CGCCGGTTTA**P**TTTTCGCG5′	312 (313)	-	-
b.) A*D*T/**P**AT (Y = *D*)		310 (309)	-2 (-4)	2.72 (5.4)
c.) TUA/TA**P** (Y = U)	5′GCGGCCAATYAAAAAGCGC3′ 3′CGCCGGTT**P**ATTTTTCGCG5′	314 (314)	-	-
d.) T*D*A/TA**P** (Y = *D*)		311 (310)	-3 (-4)	1.24 (1.78)
VI. "Random" sequence context				
a.) AUA'/T**P**T' (X = U)	5′CGTACATAXACCTAGCAGC3′ 3′GCATGTAT**P**TGGATCGTCG5′	315 (315)	-	-
b.) A*D*A'/T**P**T' (X = *D*)		311 (311)	-3.5 (-4)	1.8 (5.1)
VII. Control, (**P** two bases 3' of site)				
a.) UA**P**/TTA (X = U)	5′GCGGCCAAAXA**P**AAAGCGC3′ 3′CGCCGGTTTATTTTTCGCG5′	315 (315)	-	-
b.) *D*A**P**/TTA (X = *D*)		314 (315)	-1 (0)	1.04 (0.91)

[a]The nomenclature for the oligonucleotides reflects the three base sequence surrounding the AB site (or uracil) on each strand. The nucleotides are listed in the 5′ to 3′ direction on each strand (i.e. AUA/T**P**T = 5′-AUA-3′/5′-T**P**T-3′). The average fluorescence emission maximum for all the duplexes was 370 ± 2 nm under all conditions tested.

[b]These excitation maxima were determined from first derivative plots of the excitation spectra at 25°C in TN buffer. The values in parentheses are in the presence of 15 mM $MgCl_2$.

[c]Difference between the maximal wavelength for excitation (λ_{em} = 370 nm) for the indicated AB DNA and the corresponding normal duplex [$\Delta\lambda_{max} = \lambda_{max}$ (AB-DNA) – λ_{max} (duplex)]. The values in parentheses are in the presence of 15 mM $MgCl_2$.

[d]The ratio of the fluorescence intensities at 370 nm for the abasic (F_{AB}) and parent normal duplex (F_{dup}) in TN buffer at 25°C. The values in parentheses are in the presence of 15 mM $MgCl_2$.

[e]**P**, 2-AP deoxyribonucleotide; [f]U, uridine deoxyribonucleotide; [g]*D*, deoxyribose aldehyde AB site; [h]*F*, 3-hydroxy-2-(hydroxymethyl)tetrahydrofuran AB site analog (39,40).

$$F = (F_f - F_o)\,[M^{2+}]_{free}/K_{app} + [M^{2+}]_{free} \quad \mathbf{1}$$

fluorescence intensity is assumed to be a linear function of the extent of binding, where F_o and F_f are the fluorescence intensities at zero and saturating concentrations of divalent cation, respectively. Under conditions of the experiments, $[M^{2+}]_{tot} \sim [M^{2+}]_{free}$ because [DNA phosphates] << $[M^{2+}]_{tot}$. In calculating $[M^{2+}]_{free}$, the [EDTA] = 0.1 mM that was present in TN buffer was first subtracted. In the calcium binding experiments, there was no evidence for DNA precipitation as judged by solution turbidity or by an increase in light scattering.

For determining the dissociation constant of UDG for A*F*A/T**P**T AB DNA, a 1 μM solution of the duplex DNA was titrated with increasing amounts of UDG. For this experiment, an excitation wavelength of 320 nm was used to minimize background fluorescence from tryptophan residues of the enzyme. The binding data were fitted to equation **2** after subtracting the

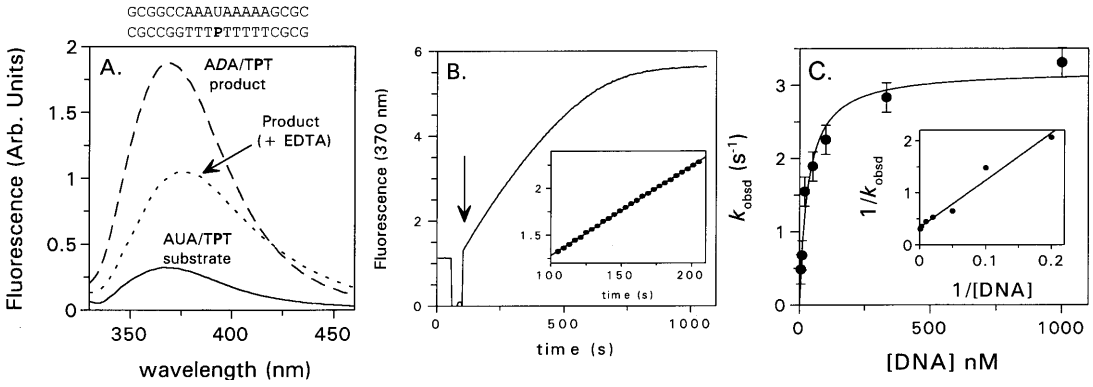

Figure 1. Differences in the fluorescence emission spectra between the substrate and AB product of the UDG reaction. (**A**) Emission spectra of the duplex substrate (sequence shown; **P** = 2-AP) and AB-DNA product (0.33 μM). The product was generated by the addition of UDG (10 nM) to the duplex substrate, and the spectrum was acquired after the completion of the reaction. (The enzyme's contribution to the fluorescence intensity is negligible in these spectra.) The fluorescence of the AB-DNA product is dependent on [Mg^{2+}], which is demonstrated by the ~50% decrease in the emission intensity of the AB-DNA at 370 nm after the addition of EDTA to 5 mM concentration. The fluorescence of the substrate duplex is not affected by the presence of Mg^{2+} (<10 % change). (**B**) Time course for the change in emission fluorescence intensity at 370 nm using 1 μM duplex DNA substrate and 0.67 nM UDG (λ_{ex} = 310 nm). The arrow indicates when the enzyme was added. (inset) Exploded linear region of the time course in (B). Conditions were: 10 mM Tris–HCl buffer at pH 8.0, 20 mM NaCl and 2.5 mM $MgCl_2$ at 25°C ('TMN buffer'). (**C**) Steady-state kinetics of UDG catalyzed *N*-glycosidic bond cleavage in TMN buffer at 25°C. Dependence of $k_{obsd} = v_{obsd}/[UDG]_{tot}$ on the concentration of the duplex substrate. The curve is a non-linear least-squares fit of the data to a hyperbolic saturation curve. The inset shows a double-reciprocal plot of the data. The rate constants derived from this data were: k_{cat} = 3.2 ± 0.15/s, K_m = 30 ± 10 nM, $k_{cat}/K_m = 1.0 \pm 0.2 \times 10^8$/M/s. The uncertainties in the kinetic parameters were taken as the standard errors of the fits, assuming that the standard deviation of the data points is approximated by the standard deviation of the points from the fitted curve.

$$F = -\{(F_o - F_f)/2*[DNA]_{tot}\}\{b - (\sqrt{b^2 - 4[UDG]_{tot}[DNA]_{tot}})\} + F_o, \quad b = K_d + [UDG]_{tot} + [DNA]_{tot} \qquad 2$$

background fluorescence of UDG from each spectrum. All binding measurements were done at 25°C using TMN buffer (10 mM Tris–HCl pH 8.0, 2.5 mM $MgCl_2$, 25 mM NaCl). The concentrations of $MgCl_2$ stocks were determined by a colorimetric chloride assay reagent obtained from Aldrich Chemical Company.

Acrylamide quenching experiments

Quenching of the fluorescence (λ_{em} = 369 nm) of 2-AP containing DNA oligonucleotides was performed by addition of increasing amounts of acrylamide to solutions of DNA in TN buffer (or TN supplemented with 15 mM $MgCl_2$) at 25°C. For measuring the fluorescence quenching of the UDG–A*F*A/T**P**T complex, UDG (20 μM) was first titrated alone to determine the background fluorescence decrease due to quenching of the tryptophan residues of the enzyme. Then the complex was titrated under the same conditions and the F_o/F ratios for the free enzyme were subtracted from those determined for the complex, where F_o and F are the fluorescence intensities in the absence and presence of the quench agent, respectively. The corrected ratios were plotted against the acrylamide concentration, and the slopes were determined by linear regression analysis.

RESULTS

DNA oligonucleotides and a new kinetic assay for UDG

The DNA oligonucleotides used in these studies and their abbreviations are indicated in Table 1. The DNA sequences containing a single dU residue in an A/T rich context were initially chosen for mechanistic studies of UDG, and provide a convenient method for generating an aldehydic AB site at a defined position. I found that cleavage of the glycosidic bond in deoxyuridine (dU) by catalytic amounts UDG results in a surprisingly large fluorescence increase when the fluorescent base 2-AP is located opposite to dU in duplex DNA (Fig. 1A). This UDG dependent fluorescence increase requires that dU be initially present in the DNA, is strongly dependent on the concentration of divalent cations in the buffer and is substantially reduced by the addition of EDTA (Fig. 1A). As shown in Figure 1B and C, this fluorescence increase can be used to conveniently monitor the kinetics of glycosidic bond cleavage and accurately determine the kinetic parameters of UDG. These initial observations indicated that the fluorescence of the AB product was significantly greater than the substrate, and that divalent cation binding to the AB product increased this effect. Here I explore the basis for these unexpected results in detail.

Divalent cation effects on the steady-state fluorescence emission spectra of AP-containing DNA

The metal ion titrations in Figure 2A show that the fluorescence emission intensity of AFA/TPT AB DNA increases ~4-fold as the concentration of Mg^{2+}, Mn^{2+} or Ca^{2+} is increased from ~0 to 15 mM , resulting in a final fluorescence intensity that is ~6–8-fold greater than the parent duplex without the AB site. Similar divalent cation effects for other 2-AP^{opp}-containing AB DNA molecules were measured, and the ratios of their fluorescent intensities relative to that of the corresponding parent duplex (F_{AB}/F_{dup}) are reported in Table 1. In contrast, much smaller fluorescence enhancements were observed when 2-AP was placed adjacent to the AB site (see F_{AB}/F_{dup} ratios in Table 1), and *no* change was seen in the control AB DNA with 2-AP placed two nucleotides 3′ of the AB site (*DA***P**/TTA, Table 1). The parent duplexes without the AB site also show little or no change in fluorescence intensity when $MgCl_2$ is added (spectra not shown).

The fluorescence increase upon divalent cation binding was used to determine the apparent dissociation constants for Mg^{2+}, Mn^{2+} and Ca^{2+} in similar titration experiments (Fig. 2A, Table 2).

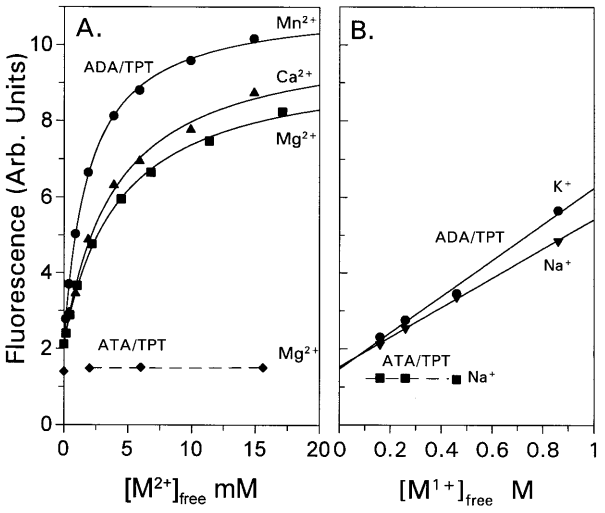

Figure 2. Titration of AP-containing AB DNA oligonucleotides with divalent and monovalent salts at 25°C. (**A**) Plot of the fluorescence intensity at 370 nm against [metal ion] for titrations of A*D*A/T**P**T AB DNA, and the ATA/T**P**T normal duplex with Mn^{2+}, Ca^{2+} and Mg^{2+}. (**B**) Emission intensity of the A*D*A/T**P**T AB duplex and the ATA/T**P**T normal duplex as a function of [monovalent salt] in TN buffer.

The binding data fit well using equation **1**, which describes binding to a single class of sites. It should be noted that the observed dissociation constants are influenced by both polyelectrolyte effects (22), and any changes in structure that occur upon ion binding. These effects are not separated in the present analysis. Also, the binding data do not necessarily indicate that the AB site is the binding site for the metal ion, because the change in environment of the 2-AP base could result from conformational effects due to global binding of metal ions to the phosphate backbone. Nevertheless, these dissociation constants are in a physiologically relevant range, and should correctly reflect the levels of metal binding. Increasing the monovalent salt concentration also resulted in a linear increase in fluorescence of 2-AP containing AB DNA, although 150–200-fold higher concentrations were required to achieve the same maximal enhancements seen with divalent metal ions (Fig. 2B). In contrast, the fluorescence of the corresponding normal duplex was unaffected by monovalent or divalent salts (ATA/T**P**T, Fig. 2A and B).

Table 2. Apparent dissociation constants of divalent cations for aldehydic and tetrahydrofuran AB DNA duplexes and maximum fluorescence changes

AB DNA	K_d^{app} (mM)			Maximum change F_{max}/F_o [a]		
	Mg^{2+}	Mn^{2+}	Ca^{2+}	Mg^{2+}	Mn^{2+}	Ca^{2+}
AFA/TPT	5.1 ± 0.5	2.1 ± 0.1	3.3 ± 0.1	4.6 ± 0.2	5.9 ± 0.2	5.0 ± 0.2
ADA/TPT	4.2 ± 0.3	1.9 ± 0.1	3.9 ± 0.5	3.5 ± 0.2	4.2 ± 0.2	3.9 ± 0.2

[a]F_{max} and F_o are the fluorescence intensities of the AB DNA duplexes in the presence and absence of saturating [divalent cation], respectively.

To rule out that the AB site or metal ions introduce a global distortion of the B-DNA structure such as a transition from B- to Z-DNA, CD spectra were acquired. In general, the normal and AB DNA spectra had a minimum at 250 ± 1 nm and a maximum at 284 ± 1 nm with a ratio A^{284}/A^{250} ~0.64, indicating that these DNA molecules are of the B-DNA type (23). No significant changes in the CD spectra of the normal or AB DNA molecules were observed upon addition of $MgCl_2$ (15 mM final concentration), or varying the temperature in the range 5–25°C (not shown).

Thus I conclude that (i) the change in environment of the 2-AP base that is induced by divalent cation binding is only seen for duplex DNA containing an AB site, (ii) the magnitude of the metal ion induced fluorescence change is greatest for 2-AP^{opp}, and (iii) a localized conformational change at the AB site is being detected.

Effects of $MgCl_2$ and temperature on base stacking of 2-AP^{opp}

The excitation spectrum of 2-AP containing DNA potentially contains two independent measures of the environment of the 2-AP base. First, the primary excitation peak of 2-AP is very sensitive to solvent exposure, and can red-shift by as much as 8 nm from its solvent exposed value (~308 nm), when the base is in a stable stacked conformation in normal duplex DNA (24–27). Second, an excitation band in the 260–280 nm region of the excitation spectrum also indicates a stacked conformation. This band arises from singlet–singlet excitation energy transfer from adjacent DNA bases to the 2-AP base, and is diagnostic for base stacking (26). Thus, this energy transfer band, and its dependence on temperature or divalent cation concentration, can provide a direct signal to monitor the influence of these parameters on the base stacking interactions of 2-AP.

The normalized fluorescence excitation spectrum of the ATA/T**P**T duplex at 25°C in TN buffer shows a red-shifted primary excitation peak at 318 nm, and a second strong excitation band in the 260–290 region indicating that the 2-AP base is shielded from the solvent, and stacked within the helix (dashed line Fig. 3A). The shape of the excitation spectrum for ATA/T**P**T was unaffected by temperature or divalent cation concentration (not shown).

In contrast, when the temperature or $[Mg^{2+}]$ is increased, the A*F*A/T**P**T AB duplex shows significant changes in the shape of its excitation spectrum indicating decreased base stacking of 2-AP^{opp}. Increasing the temperature from 5 to 40°C results in a blue shift of the direct excitation maximum, and the complete disappearance of the energy transfer band in the 260–290 nm range (Fig. 3B). Increasing the Mg^{2+} concentration from 0 to 16 mM at 25°C produces similar changes in the excitation spectra (compare Fig. 3A and B). Thus, at high temperature and high $[Mg^{2+}]$ the equilibrium shifts towards a less stacked conformation of 2-AP^{opp}. Similar effects of temperature and $[MgCl_2]$ on the excitation spectra of the other AB DNA molecules with 2-AP opposite to the AB site were also observed (not shown).

Acrylamide quenching studies

To further assess the environment of the 2-AP base in the presence and absence of metal ions, acrylamide quenching studies were performed on single-stranded, AB and normal duplex DNA molecules, as well as AB DNA bound to UDG (see below).

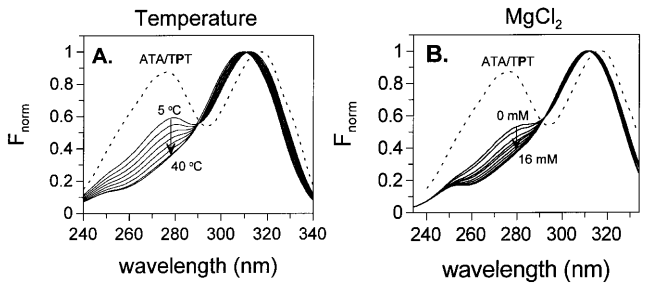

Figure 3. Fluorescence excitation spectra of 2-AP^{opp} as a function of temperature and [$MgCl_2$]. (**A**) Temperature dependence of the excitation spectrum of A*F*A/T**P**T AB DNA (solid line) in TN buffer. Spectra were acquired from 5 to 40°C in increments of 5°C. The excitation spectrum of the ATA/T**P**T normal duplex (dashed line) at 25°C in TN buffer is shown for comparison. The spectra are normalized to a peak amplitude of one. (**B**) Excitation spectra of the A*F*A/T**P**T AB duplex as a function of increasing concentration of $MgCl_2$ (0–16 mM). The excitation spectrum of the ATA/T**P**T normal duplex (dashed line) at 25°C in TN buffer is shown for comparison.

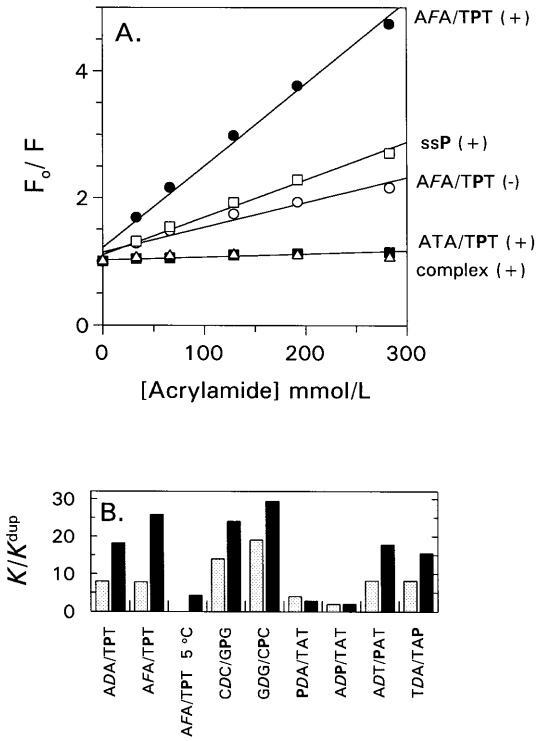

Figure 4. Acrylamide quenching studies of 2-AP containing DNA. (**A**) Concentration dependence of the quenching effects of acrylamide on the 2-AP containing DNA molecules in the presence (+) and absence (–) of 15 mM $MgCl_2$ at 25°C (see Table 1 for DNA abbreviations). The UDG•A*F*A/T**P**T complex data was collected on a 1 µM solution of A*F*A/T**P**T AB DNA containing 20 µM UDG. (**B**) Slopes of the Stern–Volmer plots for each DNA relative to that of the normal ATA/T**P**T duplex. The relative sensitivity to the quench (K/K^{dup}) is defined as the slope for the indicated DNA (K) divided by the slope measured for ATA/T**P**T (K^{dup}).

In Figure 4A, the concentration of acrylamide is plotted against the ratio F_0/F, where F_0 and F are the fluorescence intensities in the presence and absence of added quenching agent. The slopes (K) of these Stern–Volmer plots are proportional to the accessibility of the quenching agent to the 2-AP base as well as the lifetime of the excited state (28). The overall order of the measured slopes is: AB-DNA$^{opp,\ (M2+)}$ > single-stranded DNA$^{(M2+)}$ ~ AB-DNA$^{opp,\ (no\ M2+)}$ >> normal duplex DNA > UDG–AB complex.

The slopes (K) of the plots shown in Figure 4A, in addition to those obtained from other DNA molecules in Table 1, were normalized to the slopes measured for the ATA/T**P**T duplex DNA (K/K^{dup}), and these ratios are shown as bar graphs in Figure 4B. The data in Figure 4B show that the fluorescence of the AB-AP^{opp} is 18–30-fold more sensitive to the quenching agent than the normal ATA/T**P**T duplex in the presence of 15 mM Mg^{2+}, and is ~8-fold more sensitive in the absence of Mg^{2+}. The sensitivity of the fluorescence of AB-AP^{opp} abasic DNA to the quenching agent drops 6.2-fold at 5°C (see A*F*A/T**P**T, Fig. 4B), consistent with the excitation energy transfer band which indicated a stacked conformation under these conditions (Fig. 3A). In contrast, 2-AP^{adj} (the 2-aminopurine base located adjacent to the abasic site on either strand) duplexes (**P***D*A/TAT and A*D***P**/TAT, Fig. 4B) have a lower relative sensitivity to the quenching agent, both in the presence and absence of Mg^{2+}. This argues against a non-specific increase in accessibility to the quench due to phosphodiester charge neutralization by $MgCl_2$.

Base sequence effects on the stacking interactions near AB sites

On the basis of the suggestion that guanine bases flanking AB sites promote unstacking of the base opposite to the site (14), the fluorescence properties of AB duplexes in which G or C bases were placed in the positions flanking the AB site were investigated (see G*D*G/C**P**C and C*D*C/G**P**G, Table 1). The fluorescence intensity ratios (F_{AB}/F_{dup}) for these duplexes were found to be similar to the A*D*A/T**P**T AB duplex both in the presence and absence of Mg^{2+} (Table 1). The fluorescence properties of a 2-AP base located opposite to an AB site in a more random sequence context than the A/T rich duplexes tested above was also investigated, with similar results (A*D*A'/T**P**T', Table 1). Therefore, the similar fluorescence intensity ratios of AB duplexes with purine and pyrimidine bases flanking the site, regardless of the sequence, suggests that 2-AP^{opp} is in a similar environment for all these sequences, and is less stacked than in the corresponding normal duplex.

The differences between the 2-AP primary excitation maxima ($\Delta\lambda_{max}$) for nine different AB DNA molecules and their corresponding normal duplexes, are shown in Table 1. In general, these data show that the AB DNA molecules with 2-AP^{opp} have blue shifted excitation maxima, indicating increased solvent exposure of 2-AP. In contrast, the AB DNA molecules with 2-AP^{adj} show either no change or red shifted excitation spectra, suggesting that the solvent exposure of bases adjacent to the site on the same strand is similar to the native duplex (see **P***D*A/TAT and A*D***P**/TAT, Table 1). Thus by all of the criteria used here, 2-AP^{opp} appears to be in a unique less stacked environment irrespective of the sequence surrounding the site.

Binding of AB-DNA to UDG

The crystal structure of human UDG bound to duplex AB-DNA and uracil shows that the uracil nucleotide is flipped-out of the helix, but that the base opposite to the uracil is intrahelical and does not interact with any groups on the enzyme (29). This

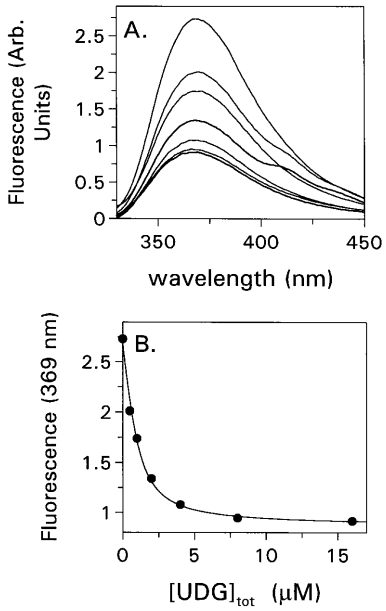

Figure 5. Binding of AB-DNA to *E.coli* UDG in the presence of $MgCl_2$. (**A**) Emission spectra of A*F*A/T**P**T AB DNA at increasing concentrations of UDG (T = 25°C, TN buffer supplemented with 2.5 mM $MgCl_2$). (**B**) Plot of fluorescence intensity at 369 nm from (A) as a function of [UDG]. The line is the non-linear least-squares fit to equation **2**.

structural result in combination with the fluorescence data reported here predicts that a fluorescence decrease should be observed when Mg^{2+}•AB-DNA binds to UDG if 2-AP^{opp} is less stacked in the free AB DNA. This prediction is substantiated by the titration data shown in Figure 5A and B. In the presence of 2.5 mM $MgCl_2$, titration of A*F*A/T**P**T AB DNA with UDG results in an ~3-fold decrease in 2-AP^{opp} fluorescence (K_d = 400 ± 90 nM). In the absence of Mg^{2+}, a slight fluorescence decrease is seen when UDG binds to A*F*A/T**P**T AB DNA, (~14%, not shown). Since the fluorescence intensity of the bound DNA is similar in the presence and absence of 2.5 mM $MgCl_2$, then the ~3-fold fluorescence decrease seen in the presence of Mg^{2+} is reasonably attributed to the effect of this cation on the conformation of 2-AP^{opp} in the free AB DNA. Thus, the enzyme shifts the equilibrium to favor a more stacked conformation for 2-AP^{opp}.

DISCUSSION

Factors determining the conformation of AB sites in DNA

The structure of AB sites in DNA has been studied in detail previously using NMR (see 14 and references therein). The most recent NMR study has shown that the AB site induces a local kink of ~30° in the duplex DNA, but that the global structural parameters of the duplex are largely those of B-DNA (14). As discussed earlier, these NMR studies performed in the absence of divalent cations suggest a high degree of flexibility at AB sites, and that the conformation of the site is highly dependent on base facing the site, and the interaction energies between bases flanking the site. As suggested by Coppel *et al.* (14) a reasonable explanation for why pyrimidine bases opposite to the AB site are sometimes found to be extrahelical is that the stronger π–π stacking interaction of purine bases flanking the site relative to pyrimidines is sufficient to kink the AB site, and expel the opposing cytosine or thymidine from the helix. Unstacked bases in duplex DNA have also been detected at A/G mismatches (30), 2-AP/G mismatches (24) and single-base bulges in DNA with similar flanking purine-induced stabilization of the stacked conformation as seen for AB sites (10,31–33). In addition, a recent NMR study has shown that the structure and stability of 2-AP:C mismatches depends on the strength of the stacking interactions between 2-AP and its flanking bases (34). Thus, base stacking interactions appear to play a key role in determining the conformation of a variety of lesion sites in DNA.

The fluorescence and quenching data presented in Figures 2–4 generally support the above NMR evidence that a high degree of flexibility exists at AB sites and base mismatches, and that the base opposite to an AB site can be significantly less stacked than in duplex DNA. However, there are two differences between the present results and those obtained from NMR data. First, there is little difference in the stacking interactions of 2-AP^{opp} (as judged by all of the spectroscopic criteria used here) when purine or pyrimidine bases flank the site. Second, in previous NMR studies it has been observed that regardless of the bases flanking the site, purine bases facing the site stack inside the helix (A), or are in a dynamic equilibrium between an intra- and extrahelical conformation (G) (see 14 and references therein). These differences may in part arise from the different DNA sequences used in this study and the NMR studies, or may indicate that the fluorescence measurements detect a partially unstacked state that is different from that observed by NMR (see below). In addition, 2-AP^{opp} may have stacking interactions more similar to guanine than adenine (35), and consistent with the NMR results, experience a dynamic equilibrium between a stacked and unstacked state. I note that in this model based on fluorescence measurements, the relatively well-stacked arrangement of the bases flanking the AB site is consistent with the proposed interactions of these bases based on NMR data (14).

In addition to the effects of base sequence and stacking interactions, it has been shown here that metal ion binding to the phosphate backbone can also disrupt the stacking interactions of the 2-AP-base with nearby DNA bases. These conclusions are supported by the ~4–6-fold increases in the fluorescence intensities of these AB DNA molecules upon metal ion binding (Fig. 2, Table 1), the metal ion induced blue shifts in the excitation spectra indicating increased solvent exposure (Fig. 3, Table 1), the temperature and divalent cation dependence of the excitation energy transfer band between normal bases and the 2-AP base (Fig. 3A and B), and the increased sensitivity of Mg^{2+}•AB-DNA to an external quenching agent (Fig. 4). To my knowledge this is the first evidence that metal ion binding to the phosphate backbone of AB DNA can provide a driving force to destabilize base stacking interactions at an AB site. This effect may simply result from compression of the phosphodiester backbone due to charge neutralization upon metal ion binding. Interestingly, compression of the phosphodiester backbone has also been suggested as a mechanism to promote base flipping by DNA repair enzymes (29).

What is the nature of the unstacked state of 2-AP in AB DNA?

The present data may be placed in a structural and dynamic framework based on previous steady-state and time-resolved

fluorescence studies on 2-AP containing DNA molecules and NMR studies on spontaneous base pair opening in duplex DNA. Steady-state fluorescence studies on normal B-DNA have shown that 2-AP, as well as other bases, exist in a temperature dependent equilibrium between stacked and less stacked states (26,37). Accordingly, fluorescence lifetime analyses of DNA typically show four lifetimes ranging from 50 to 8000 ps, with the shortest lifetime corresponding to a fully stacked state, and the longest lifetime corresponding to a small subset of 2-AP bases that are not stacked with their neighboring bases (~ 8% for 2-AP:T base pairs at 20°C; 24).

In the steady-state fluorescence experiments presented here the observed spectra are the weighted average of the populations and lifetimes of all the fluorescent states which are present. Therefore, the metal ion induced effects may reflect an increase in the population of a completely unstacked state, or a loosely associated state that has an increased solvent exposure and fluorescence lifetime as compared to the fully stacked state.

Implications for molecular recognition

The dynamic flexibility of the AB site and its average conformation could potentially enhance or inhibit recognition by DNA repair enzymes such as AB endonucleases that must interact with these sites. The intrinsic flexibility of the site could allow the AB DNA to sample conformational space without a large energetic penalty. If some of these conformations are conducive to formation of productive complexes with proteins or enzymes then specific binding or catalysis can result. In contrast, if the productive conformation is energetically inaccessible from the average conformation, then site recognition may be hindered. Indeed, we have shown here that binding of UDG to its AB DNA product proceeds by an induced-fit mechanism, where the 2-AP base opposite to the AB site becomes more stacked upon binding. This result suggests that similar transitions may occur when other enzymes bind AB sites, and could play a role in AB site recognition.

ACKNOWLEDGEMENTS

I thank Dr Morris Krauss at the Center for Advanced Research in Biotechnology for helpful discussions. This work was supported by NIH Grant GM56834 (to J.T.S.).

REFERENCES

1 Friedberg,E.C. (1985) *DNA Repair.* W.H. Freeman, New York.
2 Lindahl,T. and Nyberg,B. (1972) *Biochemistry,* **11**, 3610–3618.
3 Bailly,V. and Verly,W. (1989) *Nucleic Acids Res.*, **17**, 3617–3618.
4 Manoharan,M., Mazumder,A., Ransom.,S.C., Gerlt,J.A. and Bolton,P.H. (1988) *J. Am. Chem. Soc.*, **110**, 2690–2691.
5 Mazumder,A., Gerlt,J.A., Absalon,M.J., Stubbe,J., Cunningham,R.P., Withka,J. and Bolton,P.H. (1991) *Biochemistry,* **30**, 1119–1126.
6 Demple,B. and Harrison,L. (1994) *Annu. Rev. Biochem.*, **63**, 915–948.
7 Cuniasse,Ph., Sowers,L.C., Eritja,R., Kaplan,B., Gooodman,M.F., Cognet,J.A.H., Lebret,M., Guschlbauer,W. and Fazakerly,G.V. (1987) *Nucleic Acids Res.*, **15**, 8003–8022.
8 Cuniasse,Ph., Fazakerly,G.V., Guschlbauer,W., Kaplan,B. and Sowers,L.C. (1990) *J. Mol. Biol.*, **213**, 303–314.
9 Kalnick,M.W., Chang,C.N., Grollman,A.P. and Patel,D.J. (1988) *Biochemistry,* **27**, 924–931.
10 Kalnick,M.W., Norman,D.G., Zagorski,M.G., Swann,P.F. and Patel,D.J. (1989) *Biochemistry,* **28**, 294–303.
11 Withka,J.M., Wilde,J.A. and Bolton,P.H. (1991) *Biochemistry,* **30**, 9931–9940.
12 Singh,M.P., Hill,G.C., Péoc'h,D., Rayner,B., Imbach,J.-L. and Lown,J.W. (1994) *Biochemistry,* **33**, 10271–10285.
13 Goljer,I., Kumar,S. and Bolton,P.H. (1995) *J. Biol. Chem.*, **270**, 22980–22987.
14 Coppel,Y., Berthet,N., Coulombeau,C., Coulombeau,C. Garcia,J. and Lhomme,J. (1997) *Biochemistry,* **36**, 4817–4830.
15 Law,S.M., Eritja,R., Goodman,M.F. and Breslauer,K.J. (1996) *Biochemistry,* **35**, 12329–12337.
16 Bloom,L.B., Otto,M.R., Eritja,R., Reha-Krantz,L.J., Goodman,M.F. and Beechem,J.M. (1994) *Biochemistry,* **33**, 7576–7586.
17 Allan,B.W. and Reich,N.O. (1996) *Biochemistry,* **35**, 14757–14762.
18 McCullough,A.K., Dodson,M.L., Scharer,O.D. and Lloyd,R.S. (1997) *J. Biol. Chem.*, **272**, 27210–27217.
19 Menger,M., Tuschl,T., Eckstein,F. and Porschke,D. (1996) *Biochemistry,* **35**, 14710–14716.
20 Lindahl,T., Ljungquist,S., Siegert,W., Nyberg,B. and Sperens,B. (1977) *J. Biol. Chem.*, **252**, 3286–3294.
21 Fasman,G.D. (1975) *Handbook of Biochemistry, Nucleic Acids*, 3rd ed., Vol. 1. CRC Press, Boca Raton, FL.
22 Record,M.T., Anderson,C.F. and Lohman,T.M. (1978) *Q. Rev. Biophys.*, **11**, 103–178.
23 Simons,E.R. (1981) In Bell,J.E. (ed.), *Spectroscopy in Biochemistry,* Vol. I. CRC Press, Boca Raton, FL, pp. 84–91.
24 Guest,C.R., Hochstrasser,R.A., Sowers,L.C. and Millar,D.P. (1991) *Biochemistry,* **30**, 3271–3279.
25 Evans,K., Xu,D.-G., Kim,Y.-S. and Norlund,T.M. (1992) *J. Fluoresc.*, **2**, 209–216.
26 Nordlund,T.M., Xu,D. and Evans,K.O. (1993) *Biochemistry,* **32**, 12090–12095.
27 Xu,D., Evans,K.O. and Nordlund,T.M. (1994) *Biochemistry,* **33**, 9592–9599.
28 Bell,J.E. (1981) In Bell,J.E. (ed.), *Spectroscopy in Biochemistry,* Vol. I. CRC Press, Boca Raton, FL, pp. 183–188.
29 Slupphaug,G., Mol,C.D., Kavli,B., Arvai,A.S., Krokan,H.E. and Tainer,J.A. (1996) *Nature*, **384**, 87–92.
30 Fazakerly,G.V., Sowers,L.C., Eritja,R., Kaplan,B.E. and Goodman,M.F. (1987) *Biochemistry,* **26**, 5641–5646.
31 Kalnick,M.W., Chang,C.N., Johnson,F., Grollman,A.P. and Patel,D.J. (1990) *Biochemistry,* **28**, 3373–3383.
32 Kalnick,M.W., Norman,D.G., Zagorski,M.G., Swann,P.F. and Patel,D.J. (1990) *J. Biol. Chem.*, **265**, 636–647.
33 van den Hoogen,Y.T., van Beuzekom,A.A., van den Elst,H., van der Marel,G.A., van Boom,J.H. and Altona,C. (1988) *Nucleic Acids Res.*, **16**, 2971–2986.
34 Fagan,P.A., Fàbrega,C., Eritja,R., Goodman,M.F. and Wemmer,D.E. (1996) *Biochemistry,* **35**, 4026–4033.
35 Kollman,P.A., Weiner,P.K. and Dearing,A. (1981) *Biopolymers*, **20**, 2583–2621.
36 Nordlund,T.M., Andersson,S., Nilsson,L., Rigler,R., Gräslund,A. and McLaughlin,L.W. (1989) *Biochemistry,* **28**, 9095–9103.
37 Moe,J.G. and Russu,I.M. (1992) *Biochemistry,* **31**, 8421–8428.
38 Wu,P., Nordland,T.M., Gildea,B. and Mclaughlin,L.W. (1990) *Biochemistry,* **29**, 6508–6514.
39 Millican,T.A., Mock,G.A., Chauncey,M.A., Patel,P.T., Eaton,M.A., Gunning,J., Cutbush,S.D., Neidele,S. and Mann,J. (1984) *Nucleic Acids Res.*, **12**, 7435–7453.
40 Takishita,M., Chang,C.-N., Johnson,F., Will,S. and Grollman,A.P. (1987) *J. Biol. Chem.*, **262**, 10171–10179.